

# Electronic structure and optical spectra of $\text{YBa}_2\text{Cu}_3\text{O}_7$

S. N. Rashkeev, E. G. Maksimov, S. Yu. Savrasov, and Yu. A. Uspenskii

*Lebedev Physics Institute, USSR Academy of Sciences*

(Submitted 9 January 1990)

Zh. Eksp. Teor. Fiz. **97**, 1688–1697 (May 1990)

The dielectric constant  $\varepsilon(\omega)$ , the reflection coefficient  $R(\omega)$ , and the electron energy loss function  $\text{Im}[-1/\varepsilon(\omega)]$  are calculated by means of the band approach for the compound  $\text{YBa}_2\text{Cu}_3\text{O}_7$  at energies  $\hbar\omega \leq 40$  eV and light polarization  $\mathbf{E} \parallel a$ ,  $\mathbf{E} \parallel b$ , and  $\mathbf{E} \parallel c$ . The calculation results agree well with the direct measurements of  $R(\omega)$ , polarimetric measurements of  $\varepsilon(\omega)$ , and experiments on the fast-electron energy losses. As a rule the discrepancy between theory and experiment is less than the difference between data of various experiments. The presence of strong interband transitions is noted, including in the infrared, and they are identified. It is shown that the appreciable anisotropy of the optical properties in the  $ab$  plane for  $\hbar\omega \lesssim 4$  eV is determined mainly by electronic states localized on Cu–O(1) chains, and therefore depends strongly on the oxygen concentration.

## 1. INTRODUCTION

The electronic structure of high-temperature superconductors (HTSC), particularly compounds of the 1–2–3 type, has recently been attracting much attention and is the object of numerous investigations. Theoretical approaches to this problem can be roughly divided into three categories. First are traditional band-structure calculations based on the density-functional method with local exchange-correlation energy. According to these calculations the electron spectrum, at least near the Fermi level, is characterized by the presence of rather broad ( $W \approx 3$  eV) quasi-two-dimensional and quasi-one-dimensional bands made up of strongly hybridized  $3d$  orbitals of copper and  $2p$  orbitals of oxygen. From this point of view, the compound  $\text{YBa}_2\text{Cu}_3\text{O}_7$  is more or less a standard metal with rather weak exchange and correlation effects and with a Fermi-liquid spectrum of the elementary excitations (see the review by Pickett<sup>1</sup>).

There exists also a directly opposite view on the electronic structure of HTSC.<sup>2</sup> It is based on the model of a Mott-Hubbard dielectric in which strong intra-atomic correlations produce localized spins on the copper atoms. The interaction of spins on neighboring sites can lead to the onset of a specific state called resonant valence bonds (RVB). The properties of such a dielectric and of the metallic state that results from doping, particularly the elementary-excitation spectrum as well as the superconductivity, cannot be described in principle in the language of the single-particle Fermi-liquid excitations typical of the band picture.<sup>2</sup> There are also a large number of models of intermediate type.<sup>3,4</sup> In these the electrons on the copper, just as in the RVB, are regarded as localized by strong intra-atomic repulsion. The electrons on the copper (more accurately holes), on the other hand, are most similar to the band delocalized electrons.

The available experimental data do not lead at present to any unambiguous conclusion favoring any particular theoretical approach to the electronic structure of HTSC. For example, earlier photoemission experiments and investigations of the electron characteristic energy-loss spectrum showed rather strong deviations from the results of the band calculations (see the review by Haas<sup>5</sup>). Later studies of photoemission<sup>6,7</sup> have shown that these differences are due to a considerable extent to aging of the HTSC surface layer, in which dielectric intermediate layers are produced by the de-

crease of the oxygen content. The experimental data for freshly cleaned surface layers, however, agree quite well with the band-calculation results. The main difference between the experimental data and the calculation results is the hard shift of the emission spectrum by 1.5 eV into the region of high binding energies. Such differences are observed not only in HTSC materials, but also in many other metals, for example zinc,<sup>8</sup> and are due to inaccurate consideration of electron self-action effects in band calculations.<sup>9</sup>

Very useful in this connection are optical investigations that are much less sensitive to the state of the surface, since the depth of penetration of the light is quite large ( $> 10^3$  Å). In the first experimental investigations of the optical spectra of  $\text{YBa}_2\text{Cu}_3\text{O}_7$  the samples were ceramic polycrystals. In view of the strong anisotropy of this compound, the corresponding experimental data are difficult to interpret consistently. Measurements were recently made also on oriented films and single crystals. The experiments were performed mainly for reflection of polarized light with an electric-field vector  $\mathbf{E}$  parallel to the  $ab$  plane. The measurements were made both for crystals with twinning of the axes  $a$  and  $b$  and for single-domain sections, to cast light on the asymmetry of the optical spectra along the  $a$  and  $b$  axes. A review of the earlier investigation on the topic is contained in Ref. 10.

We present here the results of our microscopic calculations of the optical spectra of  $\text{YBa}_2\text{Cu}_3\text{O}_7$ . To obtain these spectra we first carried out a self-consistent calculation of the electronic band structure of this compound in the orthorhombic phase. The calculations were made by the standard LMTO method.<sup>11</sup> The band structure obtained agrees well with results obtained by others using a similar calculation by the LAPW method.<sup>12,13</sup>

Computations of the imaginary part of the dielectric constant (DC)  $\varepsilon_2(\omega)$  were carried out by a method described by us in detail earlier,<sup>14,15</sup> using a mesh of 242 points in  $1/8$  of the Brillouin zone. In the computation of the band energies and wave functions we used the  $s$ -,  $p$ -,  $d$ -, and  $f$ -orbitals of Y, Ba, and Cu and the  $s$ -,  $p$ -, and  $d$ -orbitals of oxygen. The integration over the Brillouin zone was by the tetrahedron method. The total number of such tetrahedra was 600. Using the function  $\varepsilon_2(\omega)$  calculated in the energy interval  $\hbar\omega \leq 40$  eV, we obtained by using the Kramers–Kronig relations the real part  $\varepsilon_1(\omega)$  of the DC, which en-

abled us to obtain readily such quantities as the optical conductivity  $\sigma(\omega) = \varepsilon_2(\omega)\omega/4\pi$ , the reflection coefficient  $R(\omega)$ , and the characteristic energy-loss energy  $L(\omega) = \text{Im}[-1/\varepsilon(\omega)]$ .

To compare the computed quantities with the experimental data, the plots of  $\varepsilon_2(\omega)$  are usually smoothed out, i.e., are convoluted with a Lorentzian of a certain width  $\gamma^{\text{inter}}$ , thus simulating the damping effects in the electronic spectrum. We used a smoothing of width  $\gamma^{\text{inter}} = 0.05 \hbar\omega$ , which enabled us to account fairly accurately for the presence or absence of a fine structure on the experimental curves in the interval  $0 \leq \hbar\omega \leq 40$  eV.

## 2. OPTICAL PROPERTIES OF $\text{YBa}_2\text{Cu}_3\text{O}_7$ IN THE ENERGY INTERVAL 0–40 eV

Figure 1 shows the results of our computations of the reflection coefficient  $R(\omega)$  for light polarization  $\mathbf{E}||a$  and  $\mathbf{E}||b$ . The same figure shows the experimental data of Ishii *et al.*<sup>16</sup> We immediately note the substantial anisotropy of  $R(\omega)$  at energies up to 4 eV. A rigorous comparison of the computed curves with the experimental data<sup>16</sup> in this region is difficult, since the measured samples were single crystals with twinning and the experimental dependence obtained corresponds to a certain averaging of curves with  $\mathbf{E}||a$  and  $\mathbf{E}||b$ . This energy region will be considered in detail in the next section. Here we pay principal attention to the region above 7 eV, where the optical properties of  $\text{YBa}_2\text{Cu}_3\text{O}_7$  are practically isotropic. At these energies the calculated  $R(\omega)$  curve agrees quite well with the experimental one. Thus, the maxima at 8.5 and 20 eV, the dip at 14 eV, and the relatively small indentations at 11 and 25 eV are reproduced. The only difference is that in the experiment the maximum at  $\hbar\omega = 8.5$  eV is approximately 1 eV higher, and the maximum at  $\hbar\omega = 20$  eV is 2 eV higher. Such a relatively small displacement of the principal maxima is typical of this energy region.<sup>15</sup>

An equally good agreement obtains also for the fast-electron characteristic loss function  $L(\omega) = \text{Im}[-1/\varepsilon(\omega)]$  (Fig. 2). This quantity was directly determined from experiments with transmission and reflection of fast electrons,<sup>17-19</sup> was obtained from ellipsometric measurements using synchrotron radiation,<sup>20</sup> and was also recalculated from measurements of the reflection coefficient.<sup>21</sup> Comparison shows that in all these experiments the same distinctive features of the function  $L(\omega)$  are observed, which are well

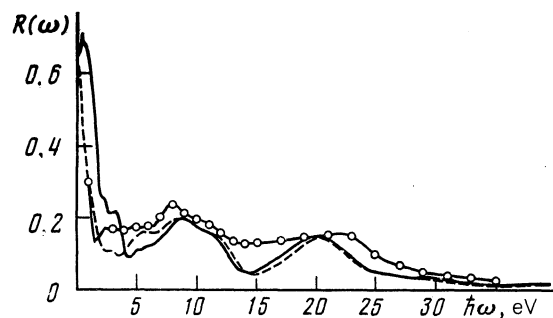


FIG. 1. Reflection coefficient of  $\text{YBa}_2\text{Cu}_3\text{O}_7$  in the energy region 0–40 eV: solid curve—calculation for  $(\mathbf{E}||b)$ , dashed—calculation for  $\mathbf{E}||a$ ; solid line with circles—experiment (data of Ref. 16).

duplicated by the calculated curve: the maxima at  $\hbar\omega = 13$  eV (in Ref. 17 the maximum at this energy is replaced by a bump) and at  $\hbar\omega = 23$  eV (in Refs. 17 and 18 it corresponds to an energy 25–26 eV), and also a maximum at  $\hbar\omega = 37$  eV (35 and 34 in the experimental papers 17 and 18 respectively). Note that the weak maximum at  $\hbar\omega = 17$  eV, observed in Refs. 17 and 18 and identified with a surface plasmon in Ref. 19, is not obtained in our calculation or in our optical measurements.<sup>20,21</sup> In addition, a high-energy plasmon with energy on the order of 1 eV was observed in experiments.<sup>17,21</sup> On the calculated curves it has an energy  $\sim 1.6$  eV at  $\mathbf{E}||c$  and  $\sim 0.8$  eV at  $\mathbf{E}||c$ .

The principal role in the formation of the optical spectrum in the high-energy region is played by two groups of innerband transitions: transitions into empty  $d$  bands of Y and Ba and into the  $4f$  band of Ba, which have an energy  $\hbar\omega \sim 7$ –12 eV, and excitation of filled oxygen  $2s$  shells with characteristic energy  $\sim 18$  eV. In addition, a definite role in the formation of the characteristic-loss spectrum is played by excitation of the filled  $4p$  shell of Ba with energy  $\sim 29$  eV. The authors of Ref. 19 assume that some influence on  $L(\omega)$  is exerted also by transitions from the filled shells of Y ( $4p$ ), Ba ( $5s$ ), and Y ( $4s$ ) with characteristic energies of order 25, 28, and 40 eV, respectively. These last three groups of electronic transitions were not taken into account in our calculation.

We conclude this section by noting that equally good an agreement with experiment<sup>16</sup> was obtained in our earlier computations<sup>22</sup> for the  $\text{La}_2\text{CuO}_4$  compound in the region  $\hbar\omega \gtrsim 3$  eV. One can conclude on this basis that there are no explicit strong correlation effects with energy scale  $\sim 5$ –10 eV in high-temperature oxide compounds. To assess the weaker correlation effects with characteristic energy of order 1–3 eV it is necessary to consider optical characteristics in the visible and infrared regions of the spectrum; this will be done in the next section.

## 3. VISIBLE AND INFRARED SPECTRAL REGIONS: ANISOTROPY OF OPTICAL PROPERTIES

We have already noted above the appreciable anisotropy of the reflection coefficient at energies  $\hbar\omega \leq 4$  eV. It is due to the presence of bands of clearly pronounced quasi-one-dimensional and quasi-two-dimensional electron motion in

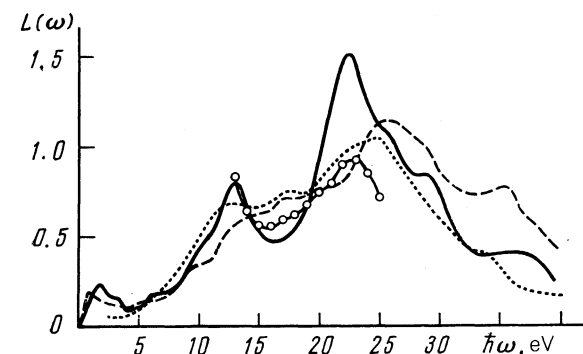


FIG. 2. Function of characteristic losses of  $\text{YBa}_2\text{Cu}_3\text{O}_7$  in the energy region 0–40 eV. Solid line—calculation for  $\mathbf{E}||a$ , dashed—experiment ( $\mathbf{E}||c$ ),<sup>17</sup> dotted—experiment ( $\mathbf{E}||c$ );<sup>18</sup> solid line with circles— $L(\omega)$  reconstructed from the data of Ref. 20 ( $\mathbf{E}||c$ ).

the electronic spectrum of  $\text{YBa}_2\text{Cu}_3\text{O}_7$  in the vicinity of the Fermi energy. Since the anisotropy of the optical properties is a very important factor for this frequency region, it is useful to consider the principal groups of the interband transitions for different light-polarization directions before a comparison is made with experiment.

Figure 3 shows the interband optical conductivity calculated for the polarizations  $\mathbf{E}\parallel a$ ,  $\mathbf{E}\parallel b$ , and  $\mathbf{E}\parallel c$  in the interval  $\hbar\omega = 0-6$  eV. At the polarization  $\mathbf{E}\parallel a$  the most interesting is the conductivity peak at  $\hbar\omega \approx 0.2$  eV, due to excitation of electrons in the  $\text{Cu}(2)-\text{O}(2)$  layers and characterized by an oscillator strength (recalculated in terms of the number of electrons per cell)  $N_{\text{eff}} = 0.04$ . In the Brillouin zone these transitions are localized along the  $SR$  direction. A similar maximum of  $\sigma(\omega)$  exists also at  $\mathbf{E}\parallel b$ . In addition, for this polarization there are also two characteristic maxima with energies 0.45 and 0.75 eV and with  $N_{\text{eff}} = 0.4$  and 0.25, respectively. Both are due to excitations of the atoms in the  $\text{Cu}(1)-\text{O}(1)$  chains. In the Brillouin zone the transitions with energy  $\hbar\omega \approx 0.45$  eV are due to a region along the  $\Gamma Z$  direction, and the transitions with energy  $\hbar\omega \approx 0.75$  eV to a region adjacent to the  $\Gamma XZU$  plane.

For the polarization  $\mathbf{E}\parallel c$  the interband transitions start out with a very low energy  $\sim 0.03$  eV. These transitions, which occupy the interval  $0.03 \leq \hbar\omega \leq 0.1$  eV and have  $N_{\text{eff}} = 0.02$ , take place between two quasi-two-dimensional zones connected with the electron motion in the  $\text{Cu}(2)-\text{O}(2)$  layers. Owing to the weak mutual influence of the two layers  $\text{Cu}(2)$  and  $\text{O}(2)$ , which make up a unit cell of the compound  $\text{YBa}_2\text{Cu}_3\text{O}_7$ , the bands are weakly split and it is just the splitting which determines the characteristic energy of the transition. Starting from the symmetry of the wave functions corresponding to these bands, it is easy also to find that these transitions have a noticeable intensity only for the  $\mathbf{E}\parallel c$  polarization.

We note also a very narrow conductivity maximum at  $\sim 0.55$  eV. It is due to excitation of the electrons in the complex  $\text{Cu}(1)-\text{O}(4)-\text{Cu}(2)$ , which forms a sort of bridge between the conducting  $\text{Cu}(1)-\text{O}(1)$  chains and the conducting  $\text{Cu}(2)-\text{O}(2)$  layers. In the Brillouin zone this transition is localized near the  $SR$  direction. Finally, the large  $\sigma(\omega)$  peak at  $\hbar\omega \approx 2.8$  eV is also due to excitations of elec-

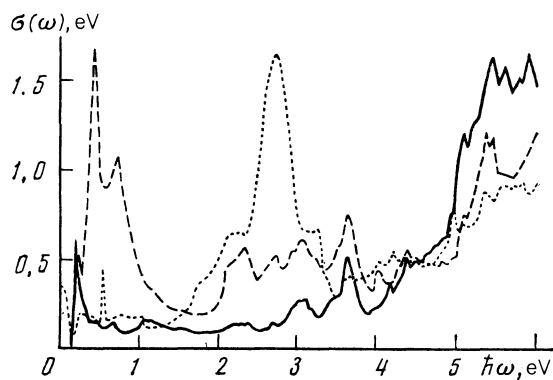


FIG. 3. Interband contribution to the optical conductivity  $\sigma(\omega)$  for three polarization directions: solid line—for  $\mathbf{E}\parallel a$ , dashed for  $\mathbf{E}\parallel b$ , dotted—for  $\mathbf{E}\parallel c$ .

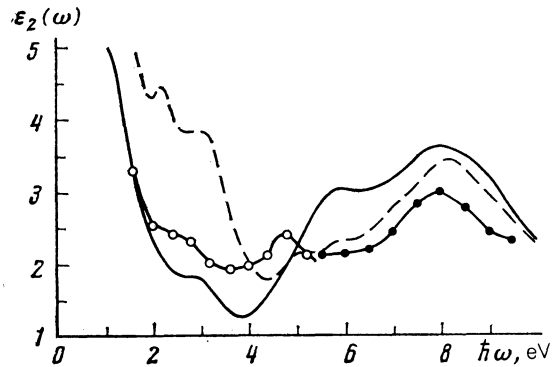


FIG. 4. Imaginary part of the dielectric constant  $\epsilon_2(\omega)$  in the region 0–10 eV: Solid line—calculation for  $\mathbf{E}\parallel a$ , dashed— $\mathbf{E}\parallel b$ ,  $\circ$ —experiment,<sup>20</sup> ( $\mathbf{E}\parallel c$ ; single crystal),  $\bullet$ —experiment<sup>20</sup> ( $\mathbf{E}\parallel c$ ; ceramic sample).

trons in the complex  $\text{Cu}(1)-\text{O}(4)-\text{Cu}(2)$  primarily to the polarization of the  $\text{O}(4)$  atom.

Concluding this description of the principal group of transitions, we note that the intraband excitations of the electrons also have a noticeable anisotropy. Thus, the intraband plasma frequency is  $\hbar\omega_p^{(a)} = 3.51$  eV for the polarization  $\mathbf{E}\parallel a$  while for  $\mathbf{E}\parallel b$  we have  $\hbar\omega_p^{(b)} = 4.20$  eV and  $\hbar\omega_p^{(c)} = 1.05$  eV.

In view of this strong difference between the electronic structures for different polarization directions, the interpretation of the experimental data obtained not only for ceramic samples but also for films oriented in the  $ab$  films and for single crystals with twinning, is quite complicated in this frequency region. Figures 4 and 5 show the  $\epsilon_2(\omega)$  and  $\epsilon_1(\omega)$  we have calculated for the polarizations  $\mathbf{E}\parallel a$  and  $\mathbf{E}\parallel b$ . The figures show also the results of ellipsometric measurements performed by the Cardona group<sup>20</sup> on twinned single crystals for  $\mathbf{E}\parallel c$  in the interval  $1.7 \leq \hbar\omega \leq 5.5$  eV and on ceramic samples in the interval  $5.5 \leq \hbar\omega \leq 9.5$  eV.

It is seen from Figs. 4 and 5 that for  $6.0 \leq \hbar\omega \leq 9.5$  eV there is very good agreement between the calculation and experiment. In the region  $4.0 \leq \hbar\omega \leq 5.5$  eV, however, the theoretical curve is shifted, so to speak, relative to the experi-

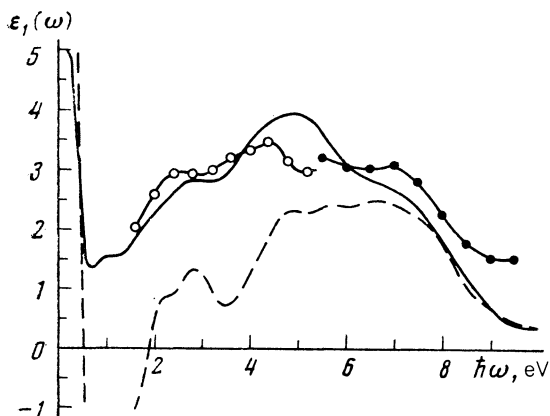


FIG. 5. Real part of dielectric constant  $\epsilon_1(\omega)$  in the region 0–10 eV; solid line—calculation for  $\mathbf{E}\parallel a$ , dashed— $\mathbf{E}\parallel b$ ,  $\circ$ —experiment<sup>20</sup> ( $\mathbf{E}\parallel c$ ; single crystal);  $\bullet$ —experiment<sup>20</sup> ( $\mathbf{E}\parallel c$ ; ceramic sample).

mental one by  $\Delta E \sim 0.3\text{--}0.5$  eV. At lower energies the positions of the main singularities of the experimental and calculated curves again agree. If we exclude the possibility of any experimental errors, the cause of the above shift of the maximum with energy  $\hbar\omega \approx 4.3$  eV can be due either to effects of corrugation of the crystal potential in the region between the atomic spheres, which are not accounted for in the present calculation, or to the insufficient accuracy of the local-density approximation for the description of the exchange-correlation potential in oxide high-temperature superconductors, or else to weak correlation effects. It is as yet difficult to state which of these causes plays the principal role here.

Figure 6 shows the  $R(\omega)$  dependences we have calculated for the polarizations  $\mathbf{E}\parallel a$  and  $\mathbf{E}\parallel b$ . Note two characteristic features. First,  $R^{(b)}(\omega)$  exceeds  $R^{(a)}(\omega)$  noticeably in the interval  $0.5 \leq \hbar\omega \leq 3$  eV. A similar relation between  $R^{(a)}(\omega)$  and  $R^{(b)}(\omega)$  was obtained for single-crystal  $\text{EuBa}_2\text{Cu}_3\text{O}_7$  in Ref. 23. To be sure, for this compound the region where  $R^{(b)}(\omega)$  exceeds  $R^{(a)}(\omega)$  noticeably was somewhat narrower—from 0.5 to 1.5 eV. A similar picture was observed also<sup>24,25</sup> for the compound  $\text{YBa}_2\text{Cu}_3\text{O}_7$  at energies  $0.1 \leq \hbar\omega \leq 2.5$  eV. Second, the  $R^{(b)}(\omega)$  curve at  $\hbar\omega \approx 0.45$  eV has a small maximum due to the peak of the interband conductivity  $\sigma^{(b)}(\omega)$ , at the same energy. A similar small maximum or bump was noted in measurements<sup>23,24</sup> made on single-domain regions of single crystals.

The position of the maximum on the experimental  $R^{(b)}(\omega)$  curves differs somewhat from the calculated data. Thus, it is observed in Ref. 23 at  $\hbar\omega \approx 0.2$  eV, as against  $\hbar\omega \approx 0.28$  eV in Ref. 24. As seen from these numbers, a difference of order 0.1 eV exists not only between experiment and our theory, but between the experimental data themselves. More significant is an observation, noted in Refs. 23 and 24 and agreeing with the results of our calculation, that the interband transitions exist only when the  $\mathbf{E}$  polarization is parallel to the  $b$  axis. More accurately, the intensity of the interband transitions with polarization  $\mathbf{E}\parallel a$  is smaller by an order of magnitude, and they are therefore hardly discernible on either the experimental or theoretical curves of  $R^{(a)}(\omega)$  curve.

Interband transitions at  $\mathbf{E}\parallel b$ , as follows from our calculations and from physical considerations, are connected with electron excitation in the copper-oxygen chain present in the  $\text{YBa}_2\text{Cu}_3\text{O}_7$  structure. This means that the energy of these transitions and their oscillator strength  $N_{\text{eff}}$  depends very critically on the oxygen content in the  $\text{YBa}_2\text{Cu}_3\text{O}_{7-x}$ . Escape of oxygen from the chain can shift the Fermi level and destroy near the Fermi level those electronic states

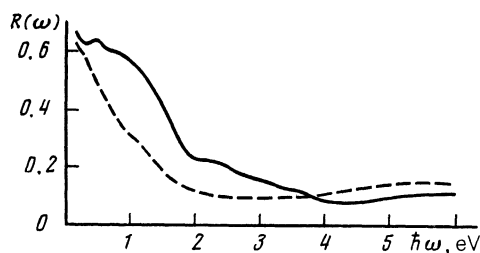


FIG. 6. Calculated reflection coefficient ( $\mathbf{E}\perp c$ ): solid line— $R^{(b)}(\omega)$  ( $\mathbf{E}\parallel b$ ), dashed— $R^{(a)}(\omega)$  ( $\mathbf{E}\parallel a$ ).

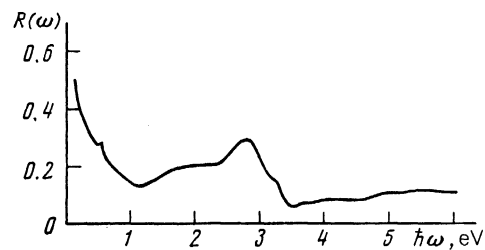


FIG. 7. Reflection coefficient of  $\text{YBa}_2\text{Cu}_3\text{O}_7$  for  $\mathbf{E}\parallel c$ .

which are connected with electrons localized on the chain. As a result, these interband transitions can be strongly altered or vanish completely. It is possible that this is the circumstance that explains the contradictory character of the experimental data at energies  $\approx 0.1\text{--}0.6$  eV.

To conclude this section we consider the behavior of  $R(\omega)$  in the polarization  $\mathbf{E}\parallel c$  (Fig. 7). Note the strong maximum of  $R(\omega)$  at  $\hbar\omega \approx 2.8$  eV, due to the large peak of the optical conductivity at the same frequency. The spectrum of the characteristic losses in the region  $0.5\text{--}3.5$  eV is also quite unique (Fig. 8). In addition to a low-energy plasmon with  $\hbar\omega \approx 0.8$  eV there exists a rather strong plasmon with energy  $\hbar\omega \approx 3$  eV, which leads to a steep decrease of the reflection coefficient at this energy (the second plasma edge). We were unable, unfortunately, to find in the literature any results of optical measurements with light polarization  $\mathbf{E}\parallel c$ .

#### 4. CONCLUSION

Let us now list the main results and conclusions of our paper. First, the peculiarities of the crystal structure of the compound  $\text{YBa}_2\text{Cu}_3\text{O}_7$ , namely, the presence of  $\text{Cu-O}$  chains in its planes, leads to a strongly pronounced anisotropy of its electronic properties, which is manifested, in particular, in an anisotropy of the optical spectra in the infrared and in the visible bands. It is important here that the calculations based on the standard wave theory in the framework of a local density functional yield not only qualitatively but also quantitative descriptions of the observed experimental data.

It should also be noted that the majority of the interband transitions in the middle IR region of the spectrum are connected mainly with electronic states in the  $\text{Cu-O}$  chain. This means that the energy and the oscillator strengths of such transitions depend very strongly on the oxygen content in the  $\text{YBa}_2\text{Cu}_3\text{O}_{7-x}$ . This circumstance apparently leads to an appreciable disparity between the available experimental data on the optical spectra at energies  $0.1 < \hbar\omega < 1$  eV, owing to the different values of the oxygen concentration  $x$ . In the

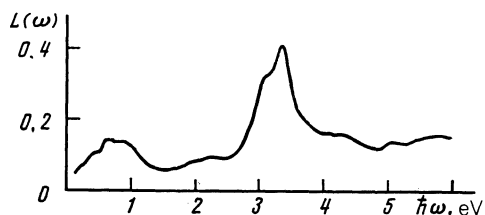


FIG. 8. Characteristic-loss function of  $\text{YBa}_2\text{Cu}_3\text{O}_7$  for  $\mathbf{E}\parallel c$ .

high-energy region  $\hbar\omega > 2$  eV, however, the agreement between the calculated and experimental optical spectra is even better than at low energies. This, in our opinion, is evidence that the band description of the electrons in  $\text{YBa}_2\text{Cu}_3\text{O}_7$  is valid and that this compound contains no specific excitations corresponding to Hubbard subbands or some other singularities that are outside the scope of the band description.

All the foregoing does not mean, of course, that the band approach in the framework of the random-phase approximation, used in the present paper, can fully describe quantitatively the behavior of the optical spectra, especially in the region of low energies at  $\hbar\omega < 0.1$  eV. It is necessary to take more accurate account, especially at low energies, of the effects of electron-phonon and electron-electron interactions and their influence on the optical spectra. This problem, however is far outside the framework of current first-principle calculations.

In conclusion, we wish to dwell briefly on the problem of antiferromagnetic ordering the systems  $\text{YBa}_2\text{Cu}_3\text{O}_6$  and  $\text{La}_2\text{CuO}_4$ . As shown by numerous calculations, the method of the density functional with local approximation for the exchange-correlation energy does not yield this state in a self-consistent manner. This circumstance is customarily used as the most weighty proof of the inapplicability of the band approach to the electron structure of HTSC. The situation is actually not so simple. First, the exact density-functional method (DFM), in accordance with the rigorous theorems pertaining to the properties of the ground state, should yield a correct description of the antiferromagnetic ordering. It can be assumed that this problem becomes solvable when more perfect exchange-correlation functionals having a nonlocal dependence on the density become available. Second, the electron excitation spectrum, and hence also the optical spectrum, of the antiferromagnetic state can in this case be poorly described in framework of the DFM. But most important, in our opinion, is the fact that the compound  $\text{YBa}_2\text{Cu}_3\text{O}_7$  is a good metal, quite far from magnetic instability. This is indeed confirmed by the results of our paper. Brief results of this paper, for the infrared region of the spectrum, were published earlier.<sup>26</sup>

The authors are deeply grateful to V. S. Bagaev, A. I. Grachev, S. M. Stishov, V. B. Timofeev, R. T. Collins, G. A.

Thomas, and A. T. Mills for fruitful discussions. One of us (E.G.M.) wishes to thank the Brookhaven National Laboratory (where this work was performed in part), and especially F. Allen, J. Davenport, and M. Strongin for hospitality.

- <sup>1</sup> W. E. Pickett, *Rev. Mod. Phys.* **61**, 433 (1989).
- <sup>2</sup> P. W. Anderson, *Science* **235**, 1196 (1987).
- <sup>3</sup> V. J. Emery, *Phys. Rev. Lett.* **58**, 2794 (1987).
- <sup>4</sup> F. C. Zhang and T. M. Rice, *Phys. Rev. B* **37**, 3759 (1988).
- <sup>5</sup> K. Haas, *Solid State Physics, Vol. 42*, ed. by H. Ehrenreich and D. Turnbull, Academic, 1989, p. 3.
- <sup>6</sup> R. S. List, A. J. Arko, Z. Fisk, *et al.* *Phys. Rev. B* **38**, 11966 (1988).
- <sup>7</sup> A. J. Arko, R. S. List, R. J. Bartlett *et al.*, *Phys. Rev. B* **22**, 4604 (1980).
- <sup>8</sup> E. J. Himpel, D. E. Eastman, E. E. Koch, and A. B. Williams, *Phys. Rev. B* **22**, 4604 (1980).
- <sup>9</sup> M. R. Norman, *Phys. Rev. B* **29**, 2956 (1984).
- <sup>10</sup> T. Timusk and D. B. Tanner, *Physical Properties of Superconductors*, D. M. Ginzberg, ed., World Scientific, 1989, p. 338.
- <sup>11</sup> O. K. Anderson, *Phys. Rev. B* **12**, 3060 (1975).
- <sup>12</sup> S. Massida, Yu. J. Freeman, and D. D. Koeling, *Physica C* **122**, 198 (1987).
- <sup>13</sup> M. Krakauer, W. E. Pickett, and R. E. Cohen, *J. Supercond.* **1**, 111 (1988).
- <sup>14</sup> Yu. A. Uspenskiĭ, E. G. Maksimov, S. N. Rashkeev, and I. I. Mazin, *Z. Phys. B* **53**, 163 (1983).
- <sup>15</sup> E. G. Maksimov, I. I. Mazin, S. N. Rashkeev, and Yu. A. Uspenskiĭ, *J. Phys. F* **18**, 833 (1988).
- <sup>16</sup> S. Tajima, H. Ishii, T. Nakahashi *et al.*, *J. Opt. Soc. Am.* **6**, 475 (1989).
- <sup>17</sup> J. Fink, N. Nücker, H. Remberg, and S. Nakai, *Proc. Int. Symp. on Electronic Structure of High- $T_c$  Superconductors*, Rome, 1988, p. 123.
- <sup>18</sup> A. Balzarotti, M. de Crescenzi, N. Motta *et al.*, *Sol. State Commun.* **68**, 381 (1988).
- <sup>19</sup> Y. Chang, M. Onellion, D. W. Miles *et al.*, *ibid.*, **63**, 717 (1987).
- <sup>20</sup> R. L. Johnson, J. Barth, M. Cardona *et al.* *Rev. Sci. Instrum.* (in press). M. Garriga, J. Humlicek, J. Barth *et al.*, *J. Opt. Soc. Amer. B* **6**, 470 (1989).
- <sup>21</sup> Xiao-lei Wang, T. Nanba, M. Ikezawa *et al.* *Japan J. Appl. Phys.* **27** L1913 (1988).
- <sup>22</sup> I. I. Mazin, E. G. Maksimov, S. N. Rashkeev, S. Yu. Savrasov, and Yu. A. Uspenskiĭ, *Pis'ma Zh. Eksp. Teor. Fiz.* **47**, 94 (1988) [*JETP Lett.* **47**, 113 (1988)].
- <sup>23</sup> J. Tanaka, K. Kamiya, and S. Tsurumi, *Physica C*, **153-155**, 653 (1988).
- <sup>24</sup> M. P. Petrov, A. I. Grachev, M. V. Krsin'kova *et al.*, *Pis'ma Zh. Eksp. Teor. Fiz.* **50**, 25 (1989) [*JETP Lett.* **50**, 29 (1989)].
- <sup>25</sup> E. V. Abel', V. S. Bagaev, D. N. Basov *et al.* *Proc. High Temp. Superconductor Physics and Material Sciences*, NATO Adv. Study Institution, Bad Windsheim, August 1989 (in press).
- <sup>26</sup> E. G. Maksimov, S. N. Rashkeev, S. Yu. Savrasov, and Yu. A. Uspenskiĭ, *Phys. Rev. Lett.* **63**, 1880 (1989).

Translated by J. G. Adashko